Synthesis and Characterization of a New Layered Ethylene-Diammonium Manganese(II) Phosphate, $(C_2N_2H_{10})Mn_2(PO_4)_2{\cdot}2H_2O$

Yanning Song, Peter Y. Zavalij, Natasha A. Chernova, and M. Stanley Whittingham*

Department of Chemistry and Institute for Materials Research, State University of New York at Binghamton, Binghamton, New York 13902-6000

Received July 18, 2003. Revised Manuscript Received October 2, 2003

A new ethylene-diammonium manganese(II) phosphate, $(C_2H_{10}N_2)Mn_2(PO_4)_2{\cdot}2H_2O$, has been synthesized hydrothermally and characterized by thermogravimetric analysis, infrared spectroscopy, and magnetic susceptibility measurements. Its crystal structure was determined by single-crystal X-ray diffraction. The compound crystallizes in the triclinic system with the noncentrosymmetric space group *P*1 and cell parameters $a = 4.910(1)$ Å, $b = 5.762(1)$ Å, $c = 9.832(2)$ Å, $\alpha = 78.11(1)°$, $\beta = 87.75(1)°$, and $\gamma = 85.63(1)°$. The manganese(II) ions form approximately square-planar layers of corner-sharing octahedra, with the layers bound by hydrogen bonds with the ammonium. The dc magnetization and ac susceptibility studies show that the compound is a 2D Heisenberg-like antiferromagnet with small additional interplanar and canting interactions. It undergoes a magnetic phase transition at 17.5(1) K; canted antiferromagnetic order is proposed for the low-temperature phase. A crossover in the critical exponent of magnetization is observed just below the transition temperature, and its possible origin is discussed.

Introduction

The widespread applications of open-framework inorganic materials in heterogeneous catalysis, separations, and ion exchange processes[1] have stimulated considerable research interest in the use of organic templates to direct the synthesis of porous materials. Since the first synthesis of microporous aluminophosphates,[2] other open-framework phosphate materials have attracted a great deal of interest. Such materials included phosphates of molybdenum,[3−4] vanadium,[5] and cobalt[6] in the early 1990s. Recently, many new phosphates of iron,[7−9] zinc,[10] and nickel[11,12] were investigated. However, there are not a lot of open-framework manganese phosphates materials reported. Up to now, only five manganese phosphates templated by organic amines or oxalates have been known,[13−16] although the possibility of the preparation of open-framework manganese phosphate had been discussed early on.[17] Two of the manganese phosphates with ethylene-diammonium templates have similar layered structures: $(C_2H_{10}N_2)Mn_2(HPO_4)_3(H_2O)$[13] and $[Mn_2(HPO_4)_3]{\cdot}(C_2H_{10}N_2)_{3/2}{\cdot}H_2PO_4$.[14] In both of these two compounds, the layers are in the formula of $[Mn_2(HPO_4)_3]^{2-}$ built up from MnO_6 octahedra and MnO_5 trigonal bipyramids and HPO_4 tetrahedra. The MnO_6 octahedra and MnO_5 trigonal bipyramids are also present in the layered piperazine compound, $Mn_6(H_2O)_2(HPO_4)_4(PO_4)_2{\cdot}C_4N_2H_{12}{\cdot}H_2O$.[15] In the oxalate compounds, $Mn_4(PO_4)_2(C_2O_4)(H_2O)_2$ and $(C_3H_{12}N_2)Mn_2(HPO_4)_2(C_2O_4)(H_2O)_2$,[16] the layers of MnO_6 octahedra and MnO_5 trigonal bipyramids are bridged by the oxalate units.

We report here the synthesis, crystal structure, and magnetic properties of a new manganese(II) phosphate: $(C_2H_{10}N_2)Mn_2(PO_4)_2{\cdot}2H_2O$, **1**. In this compound, the layers are built up with MnO_6 octahedra and PO_4 tetrahedra, related to a series of compounds with general formula $M^IM^{II}PO_4{\cdot}H_2O$ ($M^I = NH_4$, K; $M^{II} =$ Mn, Fe, Co, Ni).[18]

* Corresponding author. Phone/Fax: +1-607-777-4623. E-mail: stanwhit@binghamton.edu.

(1) Ferey G.; Cheetham, A. K. *Science* **1999**, *283*, 1125.
(2) Wilson, S. T.; Lok, B. M.; Messina, C. A.; Cannan T. R.; Flanigen, E. M. *J. Am. Chem. Soc.* **1982**, *104*, 1146.
(3) Mundi L.; Haushalter, R. C. *Inorg. Chem.* **1992**, *31*, 3050.
(4) Lightfoot P.; Masson, D. *Mater. Res. Bull.* **1995**, *30*, 1005.
(5) Soghomonian, V.; Chen, Q.; Haushalter, R. C.; Zubieta J.; O'Connor, C. J. *Science* **1993**, *259*, 1596.
(6) Chen, J.; Jones, R. H.; Natarajan, S.; Hursthouse, M. B.; Thomas, J. M. *Angew. Chem., Int. Ed. Engl.* **1994**, *33*, 639.
(7) Debord, J. R. D.; Reiff, W. M.; Haushalter R. C.; Zubieta, J. *J. Solid State Chem.* **1996**, *125*, 186.
(8) Lii, K.-W.; Huang, Y.-F.; Zima, V.; Huang, C.-Y.; Lin, H.-M.; Jiang, Y.-C.; Liao F−L.; Wang, S.-L. *Chem. Mater.* **1998**, *10*, 2599 and references therein.
(9) Song, Y.; Zavalij, P. Y.; Chernova, N. A.; Suzuki, M.; Whittingham, M. S. *J. Solid State Chem.* **2003**, *175*, 63.
(10) Song, Y.; Zavalij P. Y.; Whittingham, M. S. *J. Mater. Chem.*, **2003**, 1396 and references therein.
(11) Guillou, N.; Gao, Q.; Forster, P. M.; Chang, J. S.; Nogues, M.; Park, S. E.; Ferey, G.; Cheetham A. K. *Angew. Chem., Int. Ed.* **2001**, *40*, 2831.
(12) Chang, J. S.; Park, S. E.; Gao, Q.; Ferey, G.; Cheetham A. K. *Chem. Commun.* **2001**, 859.
(13) Escobal, J.; Pizarro, J. L.; Mesa, J. L.; Lezama, L.; Olazcuaga, R.; Arriortua, M. I.; Rojo, T. *Chem. Mater.* **2000**, *12*, 376.
(14) Chippindale, A. M.; Gaslain, F. O. M.; Cowley, A. R.; Powell, A. V. *J. Mater. Chem.* **2001**, *11*, 3172.
(15) Kongshaug, K. O.; Fjellvag, H.; Lillerud, K. P. *J. Solid State Chem.* **2001**, *156*, 32.
(16) Lethbridge, Z. A. D.; Hillier, A. D.; Cywinski, R.; Lightfoot, P. *J. Chem. Soc., Dalton Trans.* **2000**, 1595.
(17) Rajic, N.; Ristic, A.; Kaucic, V. *Zeolites* **1996**, *17*, 304.

10.1021/cm0346576 CCC: $25.00
Published on Web 11/19/2003

Experimental Section

Synthesis and Initial Characterization. Compound $(C_2H_{10}N_2)Mn_2(PO_4)_2{\cdot}2H_2O$, **1**, was hydrothermally synthesized from a mixture of 0.005 mol $MnCl_2$ (Aldrich), 0.072 mol H_3PO_4 (J. T. Baker), and 2.5 mol H_2O. Ethylenediamine (Aldrich) was added to the mixture dropwise to control pH of the solution. The mixture was sealed in a 125-mL Parr Teflon-lined stainless steel autoclave and heated at 165 °C for 15 h. At pH about 6.40, pink needles were formed, and these were identified by single-crystal X-ray diffraction as $(C_2H_{10}N_2)Mn_2(HPO_4)_3{\cdot}H_2O$, **2**, which has been reported by Escobal et al.[13] The new pink plate of **1** was obtained at higher pH, typically 8.4. To study the conversion of **2** to **1**, 0.2 g of compound **2** was fully dissolved in a mixture of 0.005 mol H_3PO_4 and 25 mL of H_2O, and the pH was adjusted to 8.2 by ethylenediamine. After 15 h of hydrothermal reaction at 170 °C, the product was identified as **1**. The purity of all the products was proved by powder X-ray diffraction on a Scintag XDS2000 $\theta-\theta$ powder diffractometer equipped with a Ge(Li) solid-state detector (Cu Kα radiation) and thermogravimetric analysis (TGA) run in air at 4 °C/min on a Perkin-Elmer TGA. The molar ratios of manganese/phosphorus were also analyzed by DCP-AES. The morphologies of these compounds were studied on a JEOL 8900 SEM.

Magnetic Measurements. The dc magnetization and ac susceptibility were measured using a SQUID magnetometer (Quantum Design MPMS XL-5). The dc magnetic susceptibility was measured in the magnetic field $H = 1000$ Oe, over the temperature range $2 \le T \le 298$ K. For the measurement of the zero-field cooled (ZFC) susceptibility, first, a remnant magnetic field was reduced to zero (actually less than 3 mOe), then the sample was cooled to 2 K, and after that an external field $H = 100$ Oe was applied. The ZFC curve was measured with increasing temperature from 2 to 20 K. The field-cooled (FC) susceptibility was measured with decreasing temperature from 20 to 2 K, in the same external field of 100 Oe. To measure the remnant magnetization, the sample was field-cooled in H = 100 Oe to $T = 2$ K, then the magnetic field was brought to zero, and the remnant magnetization was measured on heating the sample up to 20 K. Temperature dependence of ac susceptibility was measured in zero applied dc field over the temperature range $2 \le T \le 20$ K with ac field frequencies $f = 1$, 10, 100, and 1000 Hz and the driving amplitude $h = 1$ Oe.

Single-Crystal X-ray Diffraction. Single-crystal studies were performed on a Bruker Smart Apex diffractometer at room temperature (Mo Kα radiation, graphite monochromator). A full reciprocal sphere was scanned, and integral intensities were corrected for absorption effect using SADBAS software.[19] Crystal structures were solved by direct methods using SHELXS and refined using SHELXL97 software.[20] The hydrogen atoms of water molecules were located from the difference Fourier map. The O−H distances and H−O−H angles, but not the orientation of the water molecules, were constrained. The hydrogen atoms of ethylenediammonium were calculated from the carbon and nitrogen atoms. The 0*kl* reflections were excluded from the refinement due to twinning, leading to an overall *R* factor of 0.0372. Details of crystal data and refinement are reported in Table 1, with the selected atomic coordinates and thermal parameters in Table 2, and selected bond angles and distances in Table 3.

Table 1. Crystallographic Data for 1

formula	$C_2H_{14}Mn_2N_2O_{10}P_2$
fw	397.96
crystal system	triclinic
space group	*P*1
crystal size, mm	0.02 × 0.20 × 0.60
color/shape	pink/plate
a, Å	4.910(1)
b, Å	5.762(1)
c, Å	9.832(2)
α, °	78.114(3)
β, °	87.748(3)
γ, °	85.626(3)
V, Å^3	271.30(8)
Z	1
F(000)	202
D_{calc}, g·cm^{-3}	2.448
μ, mm^{-1}	2.675
$2\theta_{max}$, °	52.74
no. measured reflections	1835
no. observed reflections	1489
Flack's parameter	−0.01(3) for 543 pairs
no. refined parameters	177
R_{int}	0.0400
R_{sig}	0.0545
wR_2	0.0946
R_1 ($I > 2\sigma I$)	0.0372

Table 2. Atomic Coordinates and Equivalent Isotropic Displacement Parameters for 1

atom	*x*	*y*	*z*	U_{eq}, Å^2
Mn1	0.5383(2)	0.5155(1)	0.4777(1)	0.0130(3)
Mn2	0.0396(2)	0.0004(1)	0.5226(1)	0.0129(3)
P1	0.4868(3)	0.0801(3)	0.3192(2)	0.0105(4)
P2	0.9666(3)	0.4540(3)	0.6808(2)	0.0106(4)
O1	0.3365(9)	0.2805(9)	0.3819(5)	0.0173(11)
O2	0.3489(8)	−0.1493(8)	0.3922(5)	0.0142(10)
O3	0.7908(8)	0.0580(9)	0.3486(6)	0.0165(11)
O4	0.4464(9)	0.1210(9)	0.1633(6)	0.0190(11)
O5	0.8407(8)	0.2743(8)	0.6086(5)	0.0150(10)
O6	0.8242(8)	0.6976(8)	0.6158(5)	0.0158(10)
O7	1.2756(8)	0.4528(9)	0.6539(6)	0.0158(11)
O8	0.9122(9)	0.3980(9)	0.8362(5)	0.0176(10)
O1w	0.8709(10)	0.5825(9)	0.3144(6)	0.0188(11)
H1w	0.920(14)	0.706(8)	0.341(9)	0.028
H2w	0.993(12)	0.470(8)	0.343(9)	0.028
O2w	0.3569(9)	−0.0456(10)	0.6858(6)	0.0185(11)
H3w	0.406(13)	0.090(7)	0.696(10)	0.028
H4w	0.505(8)	−0.137(9)	0.692(10)	0.028
C1	0.0498(12)	0.7905(14)	0.0009(8)	0.0177(15)
C2	0.3584(12)	0.7285(13)	0.0016(8)	0.0177(15)
N1	−0.0123(10)	1.0150(11)	0.0468(7)	0.0185(13)
N2	0.4164(11)	0.5062(11)	−0.0492(7)	0.0193(13)

Results and Discussion

The initial pH of the reactants was found to be critical in determining the product formed, just as noted earlier for vanadium oxides.[21] Under barely acidic conditions at a pH of 6.40 needles of compound **2** are the main product, whereas under alkaline conditions where the pH exceeds 8.0 the main product is compound **1**. Chemical analysis using DCP-AES showed that the Mn/P ratios are 0.98 for **1** and 0.66 for **2**, in agreement with the chemical formulas of $(C_2H_{10}N_2)Mn_2(PO_4)_2{\cdot}2H_2O$ for **1** and $(C_2H_{10}N_2)Mn_2(HPO_4)_3{\cdot}H_2O$ for **2**. Compound **2** can be used as the starting reagent to form the higher pH compound **1**. A similar interconversion behavior is found for iron and zinc phosphate materials.[9,10]

Compound **1** loses weight in 3 steps when heated in air; as shown in Figure 1. The weight loss of 9.5% between 100 and 170 °C corresponds to the dehydration of water (calcd 9.1%). The following weight loss of 12.4% between 240 and 500 °C corresponds to the decomposition of ethylenediamine (calcd 12.8%). The final weight loss above 500 °C can be assigned to the transformation

(18) Tranqui, D.; Durif, A.; Guitel, J.-C.; Averbuch-Pouchot, M. T. *Bull. Soc. Fr. Mineral. Cristallogr.* **1968**, *91*, 10.

(19) Sheldrick, G. M. *SADABS*. University of Göttingen: Germany, 1996.

(20) Sheldrick, G. M. *SHELXL-97*. University of Göttingen: Germany, 1997.

(21) Chirayil, T.; Boylan, E. A.; Mamak, M.; Zavalij, P. Y.; Whittingham, M. S. *Chem. Comm.* **1997**, 33.

Table 3. Selected Distances (Å) and Angles (°) for 1[a]

Bond Distances (Å)			
Mn1 octahedron		Mn2 octahedron	
Mn1−O2^{i}	2.102(5)	Mn2−O3^{ii}	2.097(5)
Mn1−O7^{ii}	2.105(5)	Mn2−O5^{ii}	2.100(5)
Mn1−O1	2.123(5)	Mn2−O6^{iii}	2.132(4)
Mn1−O5	2.212(5)	Mn2−O2	2.190(5)
Mn1−O1w	2.242(5)	Mn2−O2w	2.243(5)
Mn1−O6	2.424(5)	Mn2−O1	2.434(5)
P1 tetrahedron		P2 octahedron	
P1−O4	1.521(6)	P2−O8	1.512(6)
P1−O3	1.522(4)	P2−O7	1.529(4)
P1−O1	1.545(5)	P2−O6	1.544(5)
P1−O2	1.558(5)	P2−O5	1.547(5)
Bond Angles (°)			
Mn1 octahedron		Mn2 octahedron	
O2^{i}−Mn1−O7^{ii}	95.0(2)	O3^{ii}−Mn2−O5^{ii}	94.9(2)
O2^{i}−Mn1−O1	103.3(2)	O3^{ii}−Mn2−O6^{iii}	90.2(2)
O7^{ii}−Mn1−O1	91.8(2)	O5^{ii}−Mn2−O6^{iii}	103.2(2)
O2^{i}−Mn1−O5	153.8 (2)	O3^{ii}−Mn2−O2	85.7(2)
O7^{ii}−Mn1−O5	85.6(2)	O5^{ii}−Mn2−O2	154.4(2)
O1−Mn1−O5	102.9(2)	O6^{iii}−Mn2−O2	102.4 (2)
O2^{i}−Mn1−O1w	88.9 (2)	O3^{ii}−Mn2−O2w	171.4(2)
O7^{ii}−Mn1−O1w	170.8(2)	O5^{ii}−Mn2−O2w	88.9(2)
O1−Mn1−O1w	95.5(2)	O6^{iii}−Mn2−O2w	96.5(2)
O5−Mn1−O1w	87.2(2)	O2−Mn2−O2w	87.6(29)
O2^{i}−Mn1−O6	90.3(2)	O3^{ii}−Mn2−O1	86.5(2)
O7^{ii}−Mn1−O6	86.4(2)	O5^{ii}−Mn2−O1	90.7(2)
O1−Mn1−O6	166.4(2)	O6^{iii}−Mn2−O1	166.0(2)
O5−Mn1−O6	63.6(2)	O2−Mn2−O1	63.9(2)
O1w−Mn1−O6	85.3(2)	O2w−Mn2−O1	85.8(2)
P1O_4 octahedron		P2O4 octahedron	
O4−P1−O3	109.6(3)	O8−P2−O7	108.5(3)
O4−P1−O1	111.2(3)	O8−P2−O6	110.2(3)
O3−P1−O1	111.3(3)	O7−P2−O6	111.0(3)
O4−P1−O2	109.3(3)	O8−P2−O5	111.5(3)
O3−P1−O2	110.8(3)	O7−P2−O5	110.8(3)
O1−P1−O2	104.6(3)	O6−P2−O5	104.9(3)

[a] Symmetry codes: (*i*) $x, y + 1, z$; (*ii*) $x - 1, y, z$; (iii) $x - 1, y - 1, z$.

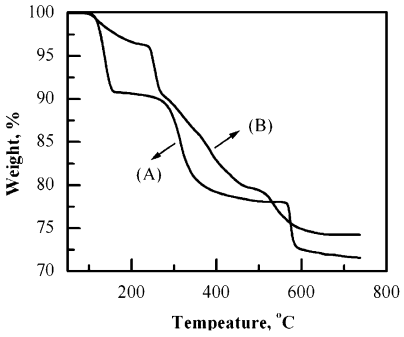

Figure 1. TGA of (a) $(C_2N_2H_{10})Mn_2(PO_4)_2{\cdot}2H_2O$ and (b) $(C_2N_2H_{10})Mn_2(HPO_4)_3{\cdot}H_2O$ in air; heating rate 4 °C/min.

of manganese phosphate to the pyrophosphate (cacld 6.4%), which was identified by powder X-ray diffraction. The decomposition of compound **2** is more complicated as shown in Figure 1. The weight loss before 200 °C is due to dehydration (3.7%; calcd 3.8%). The X-ray diffraction pattern of the residue obtained from TGA shows several peaks that can also be assigned to manganese pyrophosphate. The total weight loss of 25.8% matches the calculated value quite well assuming the final product is a mixture of $Mn_2P_2O_7$ and P_2O_5.

On the basis of the result of TGA, compound **1** was heated to 180 °C overnight. It is successfully dehydrated

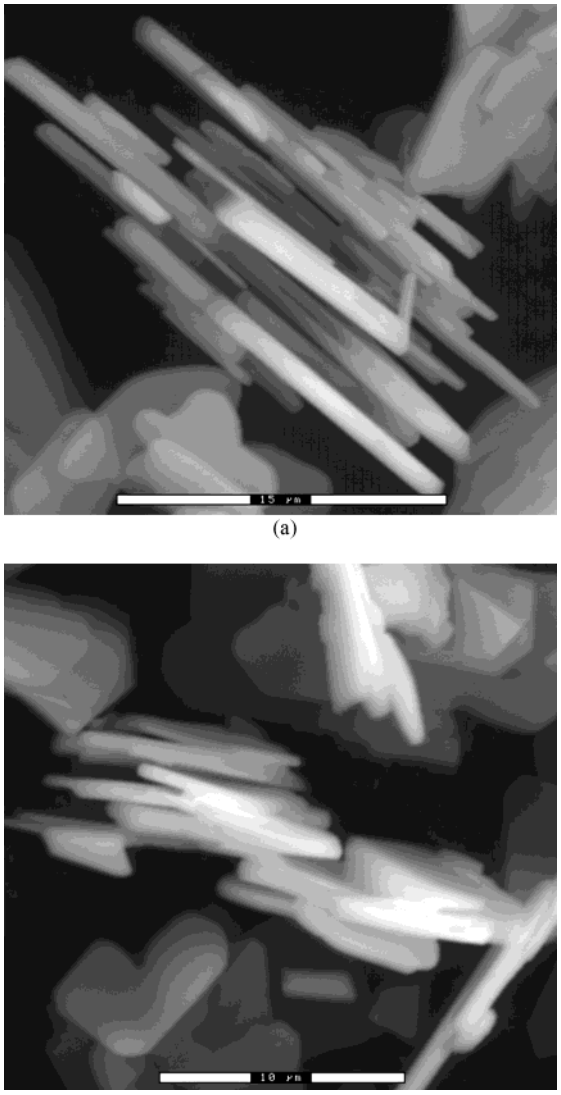

Figure 2. SEM images of compounds (a) $(C_2H_{10}N_2)Mn_2(PO_4)_2{\cdot}2H_2O$ and (b) $(C_2H_{10}N_2)Mn_2(PO_4)_2$ showing the layer morphology.

without losing amine, giving the product $(C_2H_{10}N_2)Mn_2(PO_4)_2$, **3**. The characteristic sharp peaks from amine at around 1500 cm^{-1} are present in both compounds. Interestingly, the planar morphology of **1** is maintained after calcination at 180 °C as shown in the SEM result (Figure 2). The powder X-ray patterns of **1** and **3** are shown in Figure 3. The broadening of the peaks indicates the poor crystallinity of the dehydrated compound **3**. We were not successful in the cell refinement of **3** due to peak broadening. The powder X-ray pattern of compound **1** matches the calculated pattern quite well, suggesting the high purity of the product.

Crystal Structure. There are 32 atoms in the asymmetric unit as shown in Figure 4. A PLATON[22] addsym analysis of the MnPO component of the structure did not reveal any additional symmetry elements and confirms the noncentrosymmetric group *P*1, which agrees with Flack's parameter (Table 1). PLATON free space analysis also indicates that about 25.3% of the unit cell (68.6 $Å^3$) is free space where amine resides. The two different manganese atoms in the structure are

(22) Spek, A. L. *Acta Crystallogr.* **1996**, *A46*, C34.

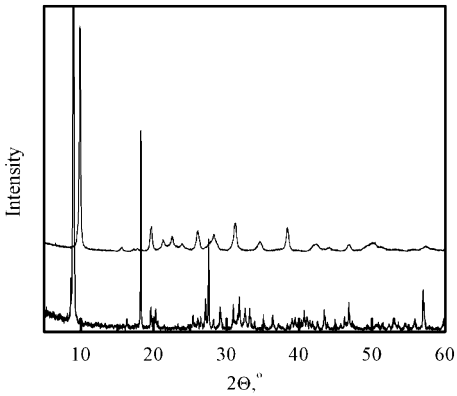

Figure 3. Powder X-ray patterns of $(C_2H_{10}N_2)Mn_2(PO_4)_2{\cdot}2H_2O$ (bottom) and $(C_2H_{10}N_2)Mn_2(PO_4)_2$ (top).

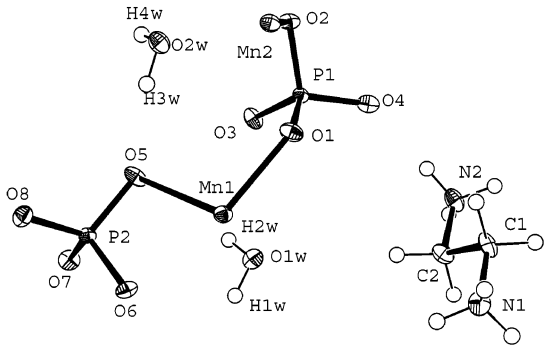

Figure 4. ORTEP view of the asymmetric unit of compound **1**; atomic displacement ellipsoids are given as 50%.

both in the +2 oxidation state as indicated by bond valence calculations:[23] 2.027 for both.

The layered compound **1** adopts the dittmarite ($NH_4MgPO_4{\cdot}H_2O$) structure.[24] It is built up from corner-sharing MnO_6 octahedra interconnected by PO_4 tetrahedra, with ethylene-diammonium cations and water molecules in the interlayer region (Figure 5a). In each layer (Figure 5b), the Mn(II) ions are coordinated in a distorted octahedron by five phosphate oxygen atoms and one water molecule. The distances of Mn1−O and Mn2−O are in the range of 2.10−2.42 Å (av = 2.20 Å) and 2.10−2.43 Å (av = 2.20 Å), respectively (Table 3). In both manganese octahedra the distance with Ow is slightly longer than the other Mn−O distances except Mn1−O6 and Mn2−O1. This means the oxygen atom is displaced away from the center of the two bridged manganese atoms. The Mn−O distance in the long edge of the center is about 2.43 Å and that in the short edge is about 2.13 Å. The cis- ∠O−Mn−O angles are in the range of 63.6−103.27° (av = 89.64°) for Mn1 and 63.85−103.16° (av = 89.67°). The PO_4 tetrahedra are more regular: the average distances of P1−O and P2−O are 1.537 and 1.533 Å, respectively. This is in good agreement with the mean value of P−O distance (1.537 Å) in phosphate minerals.[25] Each of them shares an edge and corners with three MnO_6 octahedra. Oxygen atoms of the terminal bonds of P1−O4 and P2−O8 form hydrogen bonds with water and ethylene-diammonium. Each water molecule and each ammonium group forms 3 and 4 H-bonds, respectively. However, water molecules form H-bonds in the layers, while ethylene-diammonium forms bonds with both neighboring layers binding them together. The ethylene-diammonium molecule has trans configuration with a torsion angle N1−C1−C2−N2 of −178.2(6)°.

The manganese (II) ions form approximately square-planar sheets in *ab* plane (Figure 5c). The Mn−Mn distance is in the range of 3.66−3.96 Å (av = 3.81 Å). The sum of the four Mn−Mn−Mn angles of 357° (Figure 5c) indicates good coplanarity. Similar Mn squares are also present in the ammonium compound $NH_4MnPO_4{\cdot}H_2O$ (3.795 Å) and the potassium compound $KMnPO_4{\cdot}H_2O$ (3.762 Å).[26] The distance between layers (9.6 Å) is slightly larger than those of the potassium (8.3 Å) and ammonium compounds (8.8 Å).

Unlike in the other dittmarite-like orthorhombic compounds with space group $Pmn2_1$, $NH_4MPO_4{\cdot}H_2O$ (M = Mg,[24] Co,[26] Fe,[26] Ni[27]), the title compound **1** crystallizes in triclinic space group $P1$. Probably the organic template introduces geometric constraints and lowers the symmetry. This was also found in the two magnesium compounds $(C_2H_{10}N_2)Mg_2(PO_4)_2{\cdot}2H_2O$ and $(C_4H_{14}N_2)Mg_2(PO_4)_2{\cdot}2H_2O$,[28] where the amine lowers the symmetry to monoclinic space group $P2_1/n$.

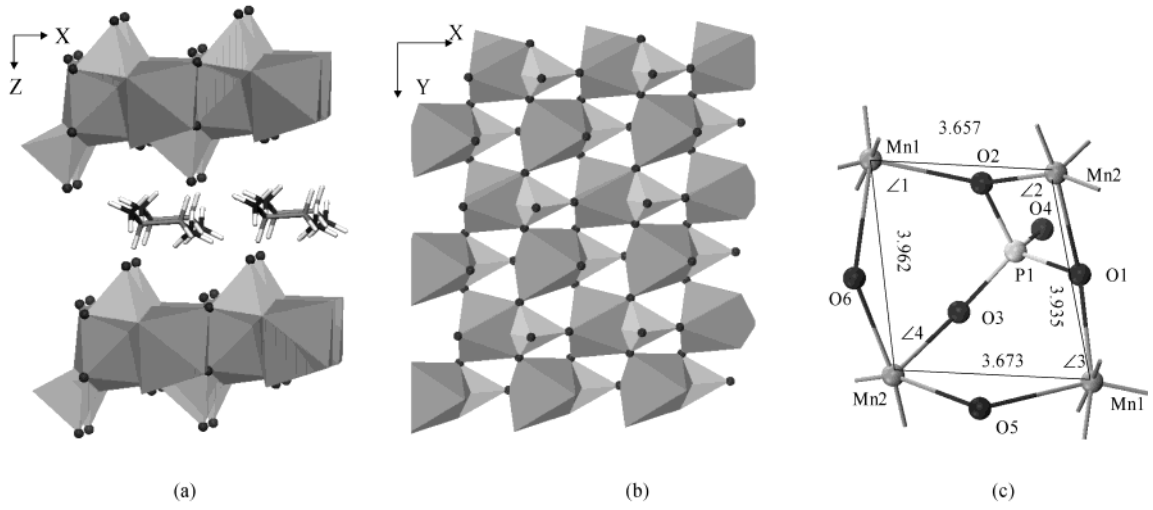

Figure 5. (a) Polyhedral view of compound 1 showing the layer structure; (b) polyhedral representation of compound **1**, showing one layer in the *xy* plane; and (c) view of a quasi-square of Mn octahedra with detailed labeling of the atoms. ∠1 = 80.124°, ∠2 = 98.675°, ∠3 = 80.30°, ∠4 = 97.911°; Mn−Mn distances are labeled.

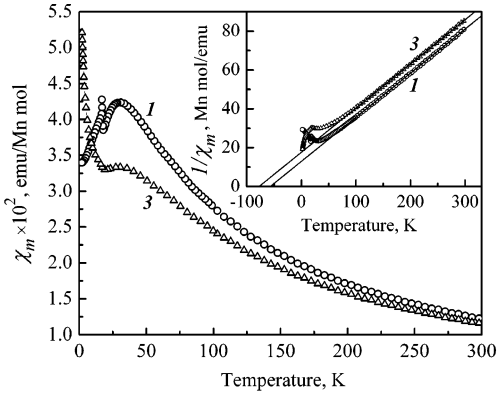

Figure 6. Temperature dependence of molar magnetic susceptibility of $(C_2H_{10}N_2)Mn_2(PO_4)_2 \cdot 2H_2O$ **1** and $(C_2H_{10}N_2)Mn_2(PO_4)_2$ **3**; the inset shows the temperature dependence of the inverse of molar susceptibility.

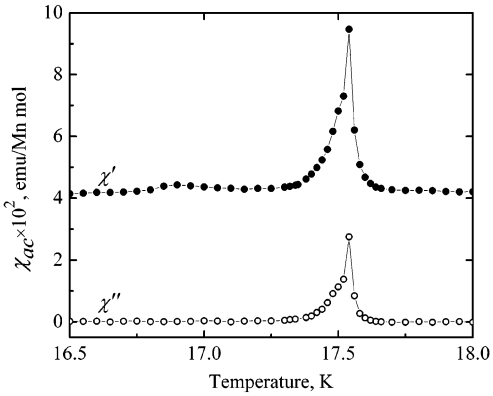

Figure 7. ac Susceptibility of **1** as function of temperature at zero dc field ($f = 100$ Hz, $h = 1$ Oe).

Magnetic Properties. The temperature dependences of the magnetic susceptibility of **1** and **3** are shown in Figure 6. At temperature above 50 K the dependences follow the Curie−Weiss law; a broad maximum typical for low-dimensional antiferromagnet is observed at about 30 K, and a sharp increase of the susceptibility, which indicates a phase transition, occurs at $T_c \approx 17.5$ K. The high-temperature parts of the curves were fitted to the Curie−Weiss law $\chi = \chi_0 + C/(T - \Theta)$ (inset in Figure 6). The temperature-independent susceptibility χ_0 was estimated as a sum of core diamagnetic susceptibilities of atoms and fixed at $\chi_0 = -1 \times 10^{-4}$ emu/mol Mn. From the values of the Curie constant C, which are equal to each other for both compounds, the effective magnetic moment of Mn^{2+} (d^5) ion 5.93 μ_B is in a very good agreement with the theoretical value. The asymptotic Curie−Weiss temperature Θ is equal to −57 K and −77 K for **1** and **3**, respectively, indicating antiferromagnetic exchange in both compounds. The stronger interactions with a higher $|\Theta|$ in the dehydrated compound can be attributed to the lattice shrinkage with dehydration, as in the iron phosphate compounds: and $\Theta = -179.8$ K for monoclinic $FePO_4$[29] and $\Theta = -70$ K for monoclinic $FePO_4 \cdot 2H_2O$.[30]

A wide maximum observed on both curves at about 30 K is indicative of low-dimensional antiferromagnetic behavior. Because manganese atoms form a quasi-square planar lattice, the experimental data may be compared to that of the 2D quadratic Heisenberg antiferromagnet lattice for spin $S = {}^5/_2$. In this model, $kT_{max}/(|J|S(S + 1)) \approx 2.05$, $\chi_{max}|J|/(Ng^2\mu_B^2) \approx 0.0551$, where T_{max} and χ_{max} are the temperature and the amplitude of the maximum.[31] From these expressions, the exchange constant is $|J|/k \approx 1.66$ K for both compounds, which is roughly the same as in $KMnPO_4 \cdot H_2O$ (−1.66 K) and $NH_4MnPO_4 \cdot H_2O$ (−1.61 K).[26] The g-factor for **1** is 1.9, in agreement with expected $g \approx 2$ for Mn^{2+}; however, in the dehydrated compound **3**, the g-factor is significantly smaller, $g \approx 1.6$, indicating inconsistence with the model chosen.

The exchange constant can also be estimated from the Curie−Weiss temperature:

$$\Theta = \frac{2S(S+1)}{3k}\sum_i Z_i J_i \qquad (1)$$

where Z_i is the number of neighbor atoms with exchange constant J_i. For the square lattice, there are four next-nearest neighbors with exchange constants $J_1/k \approx -2.4$ K and $J_1/k \approx -3.3$ K for **1** and **3**, respectively. Significant deviation between the values of the exchange constant obtained from the Θ and T_{max} may indicate that the Mn framework is not exactly 2D quadratic Heisenberg lattice with the only exchange interactions along the sides of a square. In particular, the exchange along square diagonal may be significant, leading to a frustrated magnetic configuration.

The singularities of the $\chi(T)$ dependences observed at about 17.5 K for both compounds indicate magnetic phase transitions. Sharp increase of the magnetic susceptibility of **3** below 17.5 K is typical for ferromagnetic ordering, however, the corresponding magnetic moment is too small, which points toward a weak ferromagnetism, most likely due to canting of spins. We did not perform further study of this material, as its structure is not known.

The sharp susceptibility peak defines the ordering temperature for compound **1** $T_c = 17.5(1)$. It should be noted that an ideal isotropic 2D Heisenberg system does not undergo ordering transition.[32] Occurrence of the magnetic ordering in like systems is thus attributed to the interplane interaction and/or Ising anisotropy.

In compound **1**, not only does the dc magnetization exhibit a spike at ordering temperature, but both parts of the ac susceptibility, dispersion χ' and absorption χ'' show sharp peaks (Figure 7). Such a behavior reflects formation of net magnetic moment in the ordered state, so canted antiferromagnetic order is proposed for the compound **1** below 17.5 K. This sort of ordering may appear to release frustrated magnetic interactions

(23) Brown, I. D.; Altermatt, D. *Acta Crystallogr.* **1985**, *B41*, 244.
(24) Fleischer, M. *Am. Miner.* **1972**, *57*, 1311.
(25) Huminicki, D. M. C.; Hawthorne, F. C. In *Reviews in Mineralogy and Geochemistry*, Vol. 48. Ribbe, P. H., Rosso, J. J., Eds.; Mineralogy Society of America: Washington, DC, 2002.
(26) Carling, S. G.; Day, P.; Visser, D. *Inorg. Chem.* **1995**, *34*, 3917.
(27) Goni, A.; Pizarro, J. L.; Lezama, L. M.; Barberis, G. E.; Arriortua, M. I.; Rojo, T. *J. Mater. Chem.* **1996**, *6*, 421.
(28) Kongshaug, K. O.; Fjellvag, H.; Lillerud, K. P. *J. Mater. Chem.* **2000**, *10*, 1915.
(29) Song, Y.; Zavalij, P. Y.; Suzuki, M.; Whittingham, M. S. *Inorg. Chem.* **2002**, *41*, 5778.
(30) Song, Y.; Chernova, N. A.; Zavalij, P. Y.; Whittingham, M. S. *Mater. Res. Soc. Symp. Proc.* **2003**, *755*, DD 3.9.
(31) DeJongh, L. J.; Miedema, A. R. *Adv. Phys.* **1974**, *23*, 1.
(32) Mermin N. D.; Wagner H. *Phys. Rev. Lett.* **1966**, *17*, 1133.

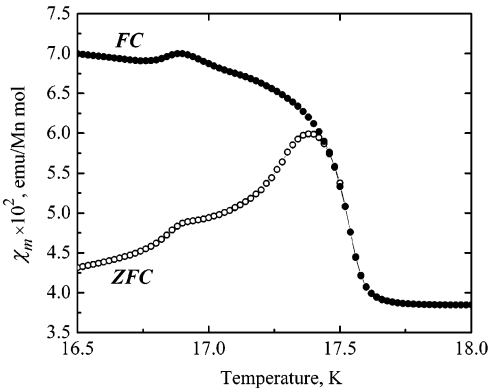

Figure 8. Field-cooled (FC) and zero-field cooled (ZFC) magnetic susceptibilities of **1**.

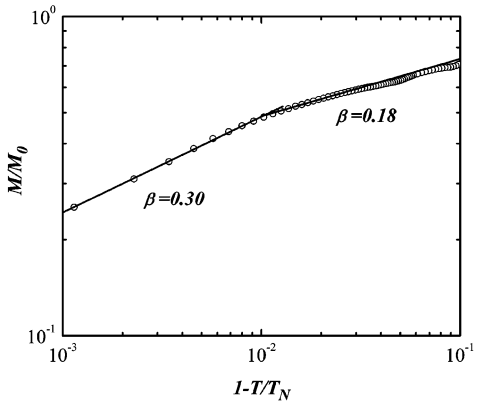

Figure 9. Double logarithmic plot of the remnant magnetization of **1** as a function of reduced temperature over the critical region; lines represent fits to the power law.

mentioned above. Canted antiferromagnetism was also found in the structurally related compounds $KMnPO_4 \cdot H_2O$ and $NH_4MnPO_4 \cdot H_2O$ based on the bulk magnetization data. The neutron powder diffraction study indicated that the canting angle was too small to be resolved, and only antiferromagnetic spin structure was reported.[26]

Below T_c, FC and ZFC susceptibilities diverge (Figure 8), which is reminiscent of spin-glass-like behavior. However, no shift of peak temperature with ac frequency was found, thus the ordered phase is simply irreversible, but not spin-glass-like. The irreversibility may be due to the formation of weak ferromagnetic domains. It is interesting to note that FC, ZFC, and dispersion curves (Figures 7 and 8) all show a bump at about 16.9 K, which may reflect a change of the domain structure by domain wall motion or domain magnetization rotation.

To study the critical behavior of compound **1**, the temperature dependence of the remnant magnetization, M_r, was measured. The remnant magnetization, being saturated at the lowest temperature, steeply decreases when the temperature is increased and drops abruptly at T_c. From the maximum of dM_r/dT, T_c is found to be 17.5(1) K, which coincides with the temperature of ac and dc susceptibilities maximum. In the critical region, $1 - T/T_c < 10^{-2}-10^{-1}$, the magnetization is governed by the asymptotic power-law with critical exponent β: $M_r = M_0(1 - T/T_c)^{\beta}$. The value of β holds information on the dimensionality and the symmetry of the magnetic sublattice undergoing ordering transition. The double logarithmic plot of the remnant magnetization as a function of the reduced temperature (Figure 9) shows the critical exponent $\beta_1 = 0.18$, which changes with another exponent $\beta_2 = 0.30$ at $T = 17.1$ K, as T_c is approached from the low-temperature side. The latter exponent is likely to correspond to one of the three-dimensional systems. The theoretical predictions are 0.31 for the Ising model, 0.33 for the XY model, and 0.35 for the Heisenberg model.[31] The value found for β_1 does not correspond to any of the tabulated values for the model magnetic systems. However, β values in a range 0.18−0.23 and a similar crossover phenomenon were found in many 2D Heisenberg-like systems,[33−37] while $\beta = 0.25$ was predicted for quadratic Heisenberg ferro- or antiferromagnets with some canting mechanism.[38]

Thus, just below the ordering temperature, correlations of critical spin fluctuations are essentially three-dimensional, whereas at lower temperature they are limited to a single layer. The crossover is observed at reduced temperature $\epsilon = 1 - T/T_c \approx 0.01$, that is, at significantly lower ϵ than in $KMnPO_4 \cdot H_2O$ and $NH_4MnPO_4 \cdot H_2O$. This confirms the known trend of ϵ decreasing as interlayer separation increases.[33]

Concluding Remarks

The manganese(II) phosphate templated by ethylenediamine with formula $(C_2H_{10}N_2)Mn_2(PO_4)_2 \cdot 2H_2O$ has been prepared under hydrothermal conditions. The single-crystal X-ray analysis shows it has a dittmarite-like structure. The manganese(II) ions form approximately square-planar layers of corner-sharing octahedra, with the layers bound by hydrogen bonds with the ammonium. The compound is a Curie−Weiss paramagnet at high temperature; below 50 K, it behaves like a 2D Heisenberg antiferromagnet on square lattice. Finally, the 3D ordering transition, driven by small interlayer exchange, is observed at 17.5 K. Canted antiferromagnetic structure is proposed for the ordered state.

Acknowledgment. This work was financially supported by the National Science Foundation through grant DMR0313963. We thank Bill Blackburn for help with the SEM study.

Supporting Information Available: Complete crystallographic, experimental, and structural data for compound **1** in CIF format. This material is available free of charge via the Internet at http://pubs.acs.org.

CM0346576

(33) Carling, S. G.; Day, P.; Visser, D. *J. Phys.: Condens. Matter* **1995**, *7*, L109.
(34) Koyama, K.; Nobumasa, H.; Matsuura, M. *J. Phys. Soc. Jpn.* **1987**, *56*, 1553.
(35) Clarke, S. J.; Harrison, A.; Mason, T. E.; McIntyre, G. J.; Visser, D. *J. Phys.: Condens. Matter* **1992**, *4*, L71.
(36) Carling S. G.; Day. P.; Visser D. *Solid State Commun.* **1993**, *88*, 135.
(37) Chernova N. A., work in progress.
(38) Kawamura H. *J. Phys. Soc. Jpn.* **1985**, *54*, 3220.